

Mapping the spatial distribution of entanglement in optical lattices

Emilio Alba,¹ Géza Tóth,^{2,3,4} and Juan José García-Ripoll¹

¹*Instituto de Física Fundamental, CSIC, Calle Serrano 113b, Madrid E-28006, Spain*

²*Department of Theoretical Physics, The University of the Basque Country, P.O. Box 644, E-48080 Bilbao, Spain*

³*IKERBASQUE, Basque Foundation for Science, E-48011 Bilbao, Spain*

⁴*Research Institute for Solid State Physics and Optics, Hungarian Academy of Sciences, P.O. Box 49, H-1525 Budapest, Hungary*

We study the entangled states that can be generated using two species of atoms trapped in independently movable, two-dimensional optical lattices. We show that using two sets of measurements it is possible to measure a set of entanglement witness operators distributed over arbitrarily large regions of the lattice, and use these witnesses to produce two-dimensional plots of the entanglement content of these states. We also discuss the influence of noise on the states and on the witnesses, as well as connections to ongoing experiments.

PACS numbers: 03.65.Mn, 42.50.Dv, 03.75.Gg

The quantum engineering of useful many-body states and the characterization of their entanglement properties are two of the most challenging areas in Quantum Information Science. In the laboratory, the creation of entangled states has been addressed in two ways. The first one starts from the control of individual quantum systems, let it be photons [1–4], neutral atoms [5, 6] or ions [7, 8], and aims at the creation of larger and larger many-body states. The second one consists of taking large numbers of these components (e.g., $10^3 - 10^6$ atoms) and studying the prepared quantum state by measuring collective quantities [9]. It thus seems that one has to make a compromise between having large entangled states or having a fine-grained knowledge of the properties of the quantum system.

In this work we show that there is an intermediate approach, by which it is possible to gain local information about a very large entangled state. More precisely, we introduce a family of operators that allow for obtaining lower bounds on the fidelity or detecting multipartite entanglement in regions of a two-dimensional graph state [10]. The witness operators presented are optimized for setups with ultracold atoms in 2D bipartite lattices, in which one now has access to the state of individual atoms [11, 12]. Remarkably, our witnesses only require the simultaneous measurement of all atoms, and with a postprocessing of the measurement statistics it provides a map of the quality and multipartite entanglement of the many-body state.

The proposed setup consists of two species of atoms trapped in two identical but independent optical potentials. For proximity with ongoing experiments we will assume that those species are actually different elements, cesium and lithium, trapped in two-dimensional triangular lattices. The lattices are generated by the projection of an appropriate mask through a powerful microscope objective [12], resulting in two potentials with similar periods that can be moved at will along the plane that confines the atoms. We will consider the two sets of

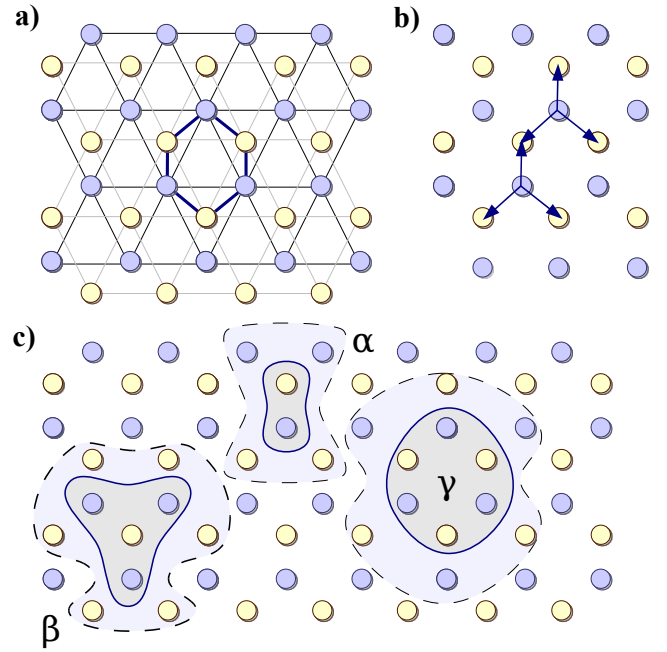


FIG. 1: (Color online) (a) We consider two species of atoms, Cs and Li, trapped in two independent triangular sublattices (blue and yellow). The combination of the two lattices can be seen as a honeycomb lattice where the atoms of Cs and Li are on different sublattices. (b) A graph state can be generated moving one of the sublattices along three different directions. (c) In this work we analyze the properties of localizable multipartite entanglement in small sets of 2 (α), 4 (β), 6 (γ), or more spins. Note that each of these small regions, Ω , has a boundary of sites, $\partial\Omega$, connected by some two-qubit interaction to the region itself.

atoms as the sublattices of a bipartite lattice enclosing all the atoms. As shown in Fig. 1a, the combination of Cs and Li triangular lattices produces a honeycomb lattice where each Cs atom is surrounded by three Li atoms, and vice versa. The bipartite nature of the lattice allows the creation of entanglement using a small number of steps,

equal to the coordination number of the full lattice. Continuing with our example, one has to move one sublattice three times so that each Cs atom approaches each of its neighboring Lithium atoms [Fig. 1b], suffering a controlled collision [13] or an engineered interaction [12]. If the lattices are very deep and the atom-atom interaction is strong enough, this can be done with a great precision.

To fix ideas, we will assume that the entangling operation between atoms in different sublattices is a CZ gate,

$$U_{CZ} = \exp\left(-i\frac{\pi}{4}\sigma_{Cs}^z\sigma_{Li}^z\right). \quad (1)$$

After three sets of operations, beginning with a product state, $(|0\rangle + |1\rangle)^{\otimes N}$, we arrive at a graph state

$$|G_{\square}\rangle \sim \prod_{i \in A} \prod_{j \in \mathcal{N}(i)} U_{CZ}^{(i,j)} (|0\rangle + |1\rangle)^{N_A + N_B}, \quad (2)$$

where A denotes the lattice of Cs, B that of Li, and $\mathcal{N}(i)$ is the set of nearest neighbors to the potential well i . Note that if instead of using the controlled-phase one implements a controlled-NOT

$$U_{CNOT} = (1 + \sigma_{Li}^z) - (1 - \sigma_{Li}^z)\sigma_{Cs}^x \quad (3)$$

where the Cs absorbs the parity of its neighbors, we obtain what we call a “parity” multipartite entangled state

$$|P_{\square}\rangle \sim \prod_{i \in A} \prod_{j \in \mathcal{N}(i)} U_{CNOT}^{(i,j)} (|0\rangle + |1\rangle)^{N_A + N_B}. \quad (4)$$

All the states that we can create using the previous operations belong to the family of stabilizer states. In both cases we have a complete set of $N_A + N_B$ local observables, the stabilizing operators, g_i , that may take values $\{-1, +1\}$, and for which the states G_{\square} and P_{\square} are eigenstates with eigenvalue $+1$ on all sites [19]. For instance, in the case of the graph state we have

$$g_i |G_{\square}\rangle = +1 |G_{\square}\rangle, \quad \forall i \in A \cup B. \quad (5)$$

with the stabilizing operators

$$g_i = \sigma_i^x \prod_{j \in \mathcal{N}(i)} \sigma_j^z. \quad (6)$$

In general, given a set of lattice sites, Ω , we can construct a projector onto a stabilizer state containing those sites

$$P_{\Omega} = \prod_{i \in \Omega} \frac{1}{2}(1 + g_i). \quad (7)$$

In theory we can use this projector to compute the fidelity of our experimentally realized mixed state, ϱ , with respect to the objective G_{\square} or P_{\square} ,

$$F_{A \cup B} = \text{tr}(P_{A \cup B} \varrho), \quad (8)$$

where the region under study now encloses the A and B sublattices. However in practice this is already impossible even for a few qubits, since the evaluation of F_{Ω} requires us to measure $2^{N_A + N_B}$ different observables coming from all possible products of the g_i operators. The difficulty of this task seems to be tantamount to performing a full tomography of the mixed state ϱ .

Instead of following this very complicated route, we will focus on two simpler questions which are intimately related: (i) a notion of local fidelity to the stabilizer state and (ii) the detection of multipartite entanglement in the lattice. In both cases we can extract a quantity, let it be a fidelity or the expectation value of an entanglement witness, which is distributed over the 2D lattice of sites. With those quantities, we can study the distribution of entanglement and how much our state has been affected by noise or decoherence.

Our notion of “localizable fidelity” builds on the fact that given a simply connected set of sites, Ω , and a perfect graph state, $|G_{\square}\rangle$, we can extract another perfect graph state in that region. One way to achieve this is measuring the boundary qubits, $\partial\Omega$ [See Fig. 1c], and depending on the outcome of those measurements, performing phase gates on the qubits which were immediately connected to them. An alternative but completely equivalent way is to disentangle the boundary with the same two-qubit unitaries we used to build the state

$$\varrho_{\Omega} = \text{tr} \left(\prod_{i \in \partial\Omega} \prod_{j \in \mathcal{N}(i)} U_{CZ}^{(i,j)} \varrho_{A \cup B} \right). \quad (9)$$

The first important remark is that this procedure still can be applied if the initial state of the atomic ensemble $\varrho_{A \cup B}$, is mixed because it decohered. The second remark is that the fidelity of the final state is related to the same observable that we found before, that is

$$F_{\Omega} = \langle G_{\Omega} | \varrho_{\Omega} | G_{\Omega} \rangle = \text{tr}(P_{\Omega} \varrho_{A \cup B}), \quad (10)$$

the fidelity of the final state only depends on how close $\varrho_{A \cup B}$ is to the eigenstates of the stabilizing operators that cover the region Ω **and** the boundary, $\partial\Omega$. The final observation is that the fidelity F_{Ω} gives us not only local information about how close our state is to the graph state, but it is also a witness for multipartite entanglement in that region, $W_{\Omega} = \frac{1}{2}\mathbb{1} - P_{\Omega}$ [14].

However, even if $\langle W_{\Omega} \rangle < 0$ detects entanglement, the evaluation of this quantity seems to require a number of measurements that increases exponentially with the number of qubits. We thus need another ingredient, which is obtained by writing the fidelity as a product of two operators constructed from stabilizing operators corresponding to different sublattices, $P_{\Omega} = P_{\Omega \cap A} P_{\Omega \cap B}$, and introducing a new operator [15]

$$\tilde{P}_{\Omega} = P_{\Omega \cap A} + P_{\Omega \cap B} - \mathbb{1} \leq P_{\Omega}, \quad (11)$$

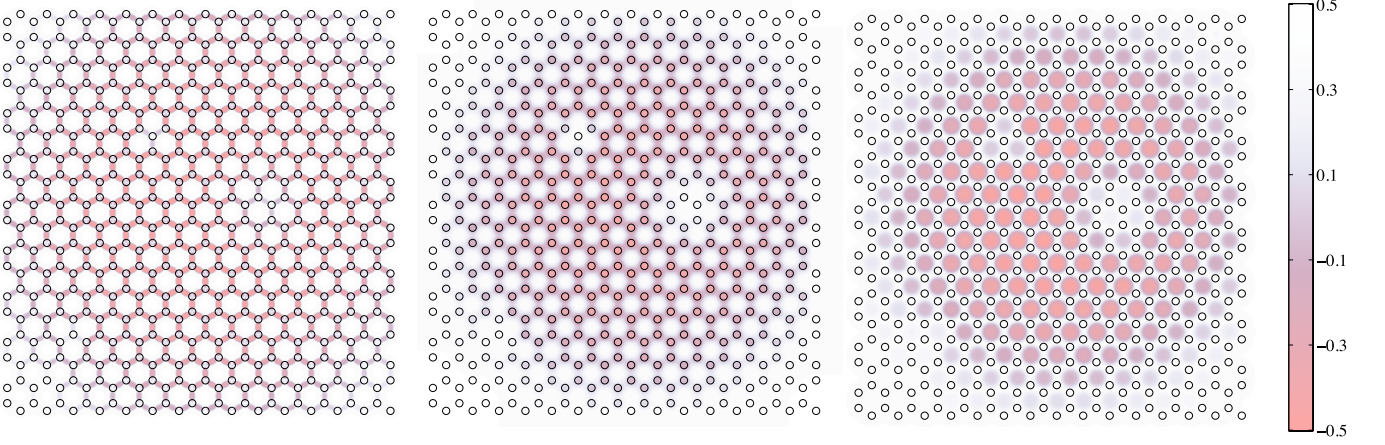


FIG. 2: (Color online) Two-dimensional distribution of the expectation values of entanglement witnesses for (left) two, (center) four and (right) six particle arrangements, α, β and γ from Fig. 1c, respectively. A negative value of the witness indicates the existence of bi- or multi-partite entanglement. All pictures present the same defects, consisting of two holes on the top-left and bottom-left regions, a circle of atoms subject to strong dephasing, and an increase of phase gate errors towards the edges of the trap.

This observable provides a lower bound for the fidelity

$$F_{\Omega} \geq \langle \tilde{P}_{\Omega} \rangle, \quad (12)$$

and is also an entanglement witness itself

$$\tilde{W}_{\Omega} = \frac{1}{2} \mathbb{1} - \tilde{P}_{\Omega}. \quad (13)$$

The advantage is that now the quantities $\langle P_{\Omega \cap A} \rangle$ and $\langle P_{\Omega \cap B} \rangle$ can be extracted from just two settings of measurements. In particular, for the graph state one such expectation values

$$\langle P_{\Omega \cap A} \rangle = \left\langle \prod_{i \in \Omega \cap A} \frac{1}{2} \left(1 + \sigma_i^x \prod_{j \in N(i)} \sigma_j^z \right) \right\rangle, \quad (14)$$

is obtained measuring σ^x in all Cs atoms ($i \in \Omega \cap A$) and σ^z in the Li ($j \in N(i)$), while the other expectation value is obtained with the opposite measurement basis. Note also that postprocessing the **same** set of measurement results we can compute the values $\langle \tilde{P}_{\Omega} \rangle$ for any region Ω , which allows us to produce two-dimensional displays of the distribution of localizable fidelity or the multipartite entanglement witness.

Next, we will consider different types of noise and will follow their action by calculating the change of $\langle g_i \rangle$. (i) Fluctuations in the energy levels of the atoms due to external fields, known as dephasing, $\epsilon_j(\varrho) = \int d\theta_j \exp(-i\sigma^z \theta_j) \varrho \exp(i\sigma^z \theta_j) p(\theta_j)$. This map is repeated on all sites, with site dependent uniformly distributed random phases in $[-\mu_j, \mu_j]$. This channel degrades the expectation value of the stabilizing operator $\langle g_i \rangle \rightarrow \langle g_i \rangle \prod_{i \in \Omega} \sin(2\mu_i)/2\mu_i$. (ii) Imperfections in the gates that entangle pairs of sites, $U_{CZ}^{(j,k)} \rightarrow$

$U_{CZ}^{(j,k)} \exp(i\theta_{jk} \sigma_j^z \sigma_k^z)$, where θ_{jk} are again random variables, uniformly distributed in $[-\mu_{jk}, \mu_{jk}]$. After a simple calculation it is easy to prove that this error amounts to a factor in the expectation value of the stabilizing operators, $\langle g_i \rangle \rightarrow \langle g_i \rangle \prod_{j \in N(i)} \frac{1}{2} (1 + \sin(2\mu_{ij})/2\mu_{ij})$. (iii) Spontaneous emission $\epsilon_{SE}(\varrho) = (1-p)\varrho + p|0\rangle\langle 0|$ and the completely depolarizing channel $\epsilon_{DP}(\varrho) = (1-p)\varrho + \frac{p}{2}\mathbb{1}$, both inducing a similar change in the expectation value of the stabilizing operator, $\langle g_i \rangle \rightarrow (1-p)\langle g_i \rangle$.

We will now calculate the degradation of the expectation value of the witness \tilde{W}_{Ω} given in Eq. (13). For that, we will take advantage of the fact that the witness is the sum of two functions of stabilizing operators corresponding to *different* sublattices. First, the degradation of $\langle P_{\Omega \cap A} \rangle$ can be obtained simply by noting that, for the noise we considered, we have $\langle P_{\Omega \cap A} \rangle = \prod_{i \in \Omega \cap A} (1 + \langle g_i \rangle)/2$ [20]. After a similar calculation for $\langle P_{\Omega \cap B} \rangle$, the expectation value of the witness Eq. (13) can be obtained. Note that it is not possible to compute so simply the change of $\langle P_{\Omega} \rangle$, since P_{Ω} contains the products of stabilizing operators of neighboring sites.

For the four types of noise and decoherence discussed above, we studied the evolution of our witness operators and the overall description of a potential experiment using them. The results are shown in Figs. 2a-c, where we plot the expectation values of $\tilde{W}_{\alpha}, \tilde{W}_{\beta}$ and \tilde{W}_{γ} . We obtain a two-dimensional map of the entanglement content, where the darkest color coincides with the bond, star or plaquette achieving maximum negative value of the witness. In these particular plots we combined all sources of decoherence, making some of them more relevant in different regions of the lattice. Overall we assumed that the phase gate is 100% accurate in the center of the lattice and acquires a 10% error at the boundary of the lattice. We also emptied certain sites, close to the bottom-left

corner and also in the top-left quadrant. These empty holes are numerically equivalent to having spontaneous emission with 100% probability. And finally we introduced a circle of strong dephasing induced by a focused laser beam over ten sites.

We can already appreciate interesting features in these simple simulations. The first one is that bipartite entanglement is less affected by noise than multiqubit arrangements. While we can reconstruct a Bell state close to the boundary with an 80% error, the four- and six-qubit states only have an appreciable value of the witness when the CZ gate is above 90% fidelity. The second feature is that the effect of local errors remains local. Thus, even though four- and six-qubit entanglement is destroyed by atom losses, away from the empty site the witnesses recover their large values, denoting the presence of multipartite entanglement.

The present study admits a straightforward generalization not only to other bipartite lattice setups, such as square lattices, but also to other interaction schemes (U_{CNOT}), or to displacing each Cs atom not three, but one or two times. First of all, if the Cs atoms move along two directions, the result is an array of linear cluster states, with an entanglement witness which is a generalization of the previous ones, and which again relies only on two-measurement settings [14]. If instead we move each Cs atom only once, then the Cs-Li interact in pairs forming a macroscopic number of disconnected two-qubit singlets. In this case we do not need a witness but can rather compute the expectation value of the projector

$$P = \frac{1}{4} (\mathbb{1} + \sigma_{\text{Cs}}^x \sigma_{\text{Li}}^x + \sigma_{\text{Cs}}^y \sigma_{\text{Li}}^z + \sigma_{\text{Cs}}^z \sigma_{\text{Li}}^y), \quad (15)$$

using three experimental settings. Finally, if we do not use a Cs lattice with unit filling, but a rather a more dilute setting, with one atom every six cells or less, the three-movement scheme should produce sets of isolated four-qubit Greenberger-Horne-Zeilinger states [16], which can be either analyzed with the previous tools, or more accurately detected using five local measurement settings [17] and no approximation.

In summary, we presented a simple scheme for detecting bipartite and multipartite entanglement in two-dimensional lattices with ultracold atoms. Our scheme only uses the fact that the lattice is bipartite and that it is possible to measure simultaneously the state of all lattice sites in each sublattice independently. This proposal represents the first experimentally realizable scheme for mapping out the entanglement distribution and fidelity of a very large many-body correlated state. It also opens the path for the experimental detection of very large cluster states, a task which so far was not achievable using ultracold atoms in optical lattices, but which becomes possible for ongoing experiments using two species of atoms and holographically generated trapping potentials [12]. Finally, we want to remark that the family of

graph states in honeycomb lattices is a universal resource for measurement-based quantum computation and that our scheme can be used to isolate regions of high fidelity in such resources.

G.T thanks the support of the National Research Fund of Hungary OTKA (Contract No. T049234), the Spanish MICINN (Consolider-Ingenio 2010 project "QOIT", project No. FIS2009-12773-C02-02) and the Basque Government (project No. IT4720-10). E.A.L. and J.J.G.R acknowledge support from the Spanish MICINN project No. FIS2009-10061 and the CAM project QUITEMAD.

-
- [1] J. Pan, D. Bouwmeester, M. Daniell, H. Weinfurter, and A. Zeilinger, *Nature* **403**, 515 (2000).
 - [2] M. Bourennane, M. Eibl, C. Kurtsiefer, S. Gaertner, H. Weinfurter, O. Gühne, P. Hyllus, D. Bruß, M. Lewenstein, and A. Sanpera, *Phys. Rev. Lett.* **92**, 087902 (2004).
 - [3] P. Walther, K. J. Resch, T. Rudolph, E. Schenck, H. Weinfurter, V. Vedral, M. Aspelmeyer, and A. Zeilinger, *Nature* **434**, 169 (2005).
 - [4] C. Lu, X. Zhou, O. Gühne, W. Gao, J. Zhang, Z. Yuan, A. Goebel, T. Yang, and J. Pan, *Nature Physics* **3**, 91 (2007).
 - [5] A. Widera, O. Mandel, M. Greiner, S. Kreim, T. W. Hänsch, and I. Bloch, *Phys. Rev. Lett.* **92**, 160406 (2004).
 - [6] M. Anderlini, P. J. Lee, B. L. Brown, J. Sebby-Strabley, W. D. Phillips, and J. V. Porto, *Nature* **448**, 452 (2007).
 - [7] H. Häffner, W. Hänsel, C. F. Roos, J. Benhelm, D. Chek-Al-Kar, M. Chwalla, T. Körber, U. D. Rapol, M. Riebe, P. O. Schmidt, et al., *Nature* **438**, 643 (2005).
 - [8] D. Leibfried, E. Knill, S. Seidelin, J. Britton, R. B. Blakestad, J. Chiaverini, D. B. Hume, W. M. Itano, J. D. Jost, C. Langer, et al., *Nature* **438**, 639 (2005).
 - [9] B. Julsgaard, A. Kozhekin, and E. S. Polzik, *Nature* **413**, 400 (2001).
 - [10] H. J. Briegel and R. Raussendorf, *Phys. Rev. Lett.* **86**, 910 (2001).
 - [11] W. S. Bakr, J. I. Gillen, A. Peng, S. Fölling, and M. Greiner, *Nature* **462**, 74 (2009).
 - [12] K.-A. B. Soderberg, N. Gemelke, and C. Chin, *New Journal of Physics* **11**, 055022 (2009).
 - [13] O. Mandel, M. Greiner, A. Widera, T. Rom, T. W. Hänsch, and I. Bloch, *Nature* **425**, 937 (2003).
 - [14] G. Tóth and O. Gühne, *Phys. Rev. Lett.* **94**, 060501 (2005).
 - [15] G. Tóth and O. Gühne, *Phys. Rev. A* **72**, 022340 (2005).
 - [16] D. Greenberger, M. Horne, A. Shimony, and A. Zeilinger, *American Journal of Physics* **58**, 1131 (1990).
 - [17] O. Gühne, C.-Y. Lu, W.-B. Gao, and J.-W. Pan, *Phys. Rev. A* **76**, 030305 (2007).
 - [18] D. Gottesman, *Phys. Rev. A* **57**, 127 (1998).
 - [19] The g_i operators are the generators of the so called stabilizer group [18].
 - [20] The Kraus decomposition of our noise channels is $\epsilon(\varrho) = \sum_k A_k \varrho A_k^\dagger$. Using the Heisenberg picture, we obtain $\langle O \rangle_{\epsilon(\varrho)} = \sum_k \langle A_k^\dagger O A_k \rangle_{\varrho}$. Furthermore, for products of stabilizing operators of sublattice A , we have $\prod_i g_{a_i} = \prod_i \sigma_{a_i}^x \times \prod_{j \in N(i)} \sigma_j^z$, where a_i are some qubits of A . For

the error channels we consider, this implies $\langle \prod_i g_{a_i} \rangle_{\epsilon(\varrho)} = \prod_i \langle g_{a_i} \rangle_{\epsilon(\varrho)}$.